Effect of long chain polyunsaturated fatty acids in the *sn*-2 position of phosphatidylcholine on the interaction with recombinant high density lipoprotein apolipoprotein A-I

Kevin W. Huggins,* Linda K. Curtiss,† Abraham K. Gebre,* and John S. Parks[1,*]

Department of Pathology,* Wake Forest University School of Medicine, Winston-Salem, NC 27157 and Departments of Immunology and Vascular Biology,† The Scripps Research Institute, La Jolla, CA 92037

Abstract The effects of polyunsaturated fatty acids (PUFA) on the structure of recombinant high density lipoprotein (rHDL) was investigated using homogeneous particles containing phosphatidylcholine (PC), [^{3}H]cholesterol, and apolipoprotein A-I (apoA-I). The PC component of the rHDL contained *sn*-1 16:0 and *sn*-2 18:1 (POPC), 18:2 (PLPC), 20:4 (PAPC), 20:5 n–3 (PEPC), or 22:6 n–3 (PDPC). The concentration of guanidine HCl ($D_{1/2}$) required to denature one-half of the apoA-I on rHDL containing long chain PUFA was reduced (1.57–1.70 m) compared to those containing POPC (2.83 m). Intrinsic apoA-I tryptophan fluorescence emission intensity and lifetimes were decreased for rHDL containing long chain PUFA compared to POPC and PLPC rHDL. Monoclonal antibody binding studies demonstrated that apoA-I had decreased immunoreactivity with monoclonal antibodies spanning amino acid residues 115–147 in rHDL containing long chain PUFA. PC lipid fluidity, measured as diphenylhexatriene (DPH) fluorescence polarization, was increased in PUFA rHDL compared to POPC rHDL. There also was a strong correlation between the number of *sn*-2 double bonds in rHDL and DPH fluorescence lifetime (r^2 = 0.89). LCAT reactivity of the homogeneous size rHDL was ordered POPC = PLPC>PAPC> PEPC>PDPC. We conclude that rHDL with long chain PUFA in the *sn*-2 position of PC contain apoA-I that is less stable and in a different conformation than that in POPC rHDL and have a fatty acyl region that is more fluid and hydrated. The weaker interaction of apoA-I with PC containing PUFA may lead to hypercatabolism of apoA-I in plasma explaining, in part, the decreased plasma HDL and apoA-I concentrations seen with PUFA diets.—Huggins, K. W., L. K. Curtiss, A. K. Gebre, and J. S. Parks. **Effect of long chain polyunsaturated fatty acids in the *sn*-2 position of phosphatidylcholine on the interaction with recombinant high density lipoprotein apolipoprotein A-I. *J. Lipid Res.* 1998.** 39: **2423–2431.**

Supplementary key words fluorescence spectroscopy • lecithin:cholesterol acyltransferase • circular dichroism • monoclonal antibodies • fluidity

Apolipoprotein A-I (apoA-I) is the predominant apolipoprotein found on high density lipoproteins (HDL). The primary sequence of apoA-I is made up of eight amphipathic α-helical repeats of 22 amino acids and two repeats of 11 amino acids (1). The presence of amphipathic α-helical repeats is hypothesized to be responsible for the ability of apoA-I to bind lipid (2). This binding occurs by the insertion of the hydrophobic face of the helix into the phospholipid monolayer, leaving the hydrophilic face exposed to the aqueous environment. ApoA-I is believed to have two major functions in plasma: *a*) providing structural stability to HDL particles, and *b*) activation of the plasma enzyme lecithin:cholesterol acyltransferase (LCAT) (1). Thus, it is generally believed that the way in which apoA-I interacts with phospholipid determines not only the structure but the physiological function of HDL (3).

Many structural studies of HDL have been carried out using recombinant HDL (rHDL). These particles consist of phospholipid, cholesterol, and apolipoprotein and are formed by cholate dialysis (4). rHDL mimic nascent HDL particles secreted by the liver with regard to size, shape, and chemical composition (5). It is believed that the rHDL exist as a lipid bilayer with an annulus of apolipoprotein concealing the hydrophobic acyl chains of the phospholipid molecules from the hydrophilic environment. Infrared spectroscopy data have suggested that the amphipathic α-helices of apoA-I lie parallel to the fatty acyl chains (6). Jonas, Kezdy, and Wald (7) have found that rHDL particle size is related to the conformation of apoA-I on the particle and that certain conformations

Abbreviations: apoA-I, apolipoprotein A-I; HDL, high density lipoprotein; LCAT, lecithin:cholesterol acyltransferase; rHDL, recombinant HDL; PUFA, polyunsaturated fatty acids; PC, phosphatidylcholine; POPC, 1-palmitoyl-2-oleoyl-*sn*-glycero-3-phosphocholine; PLPC, 1-palmitoyl-2-linoleoyl-*sn*-glycero-3-phosphocholine; PAPC, 1-palmitoyl-2-arachidonoyl-*sn*-glycero-3-phosphocholine; PEPC, 1-palmitoyl-2-eicosapentaenoyl-*sn*-glycero-3-phosphocholine; PDPC, 1-palmitoyl-2-docosahexaenoyl-*sn*-glycero-3-phosphocholine; DMS, dimethyl suberimidate; GndHCl, guanidine hydrochloride; ($D_{1/2}$), concentration of GndHCl required to denature one half of the apoA-I on rHDL; (G^0d), free energy of denaturation at zero GndHCl concentration; DPH, diphenylhexatriene.

[1] To whom correspondence should be addressed.

of apoA-I are more effective in the activation of LCAT than others.

Very little is known concerning the role different phospholipid species play in modulating rHDL structure. Zorich, Kezdy, and Jonas (8) have shown that the type of phospholipid complexed with apoA-I determines the size distribution of rHDL and the α-helical content of apoA-I. In addition, the type of phospholipid species appears to influence LCAT reactivity through effects at the active site as well as through interfacial effects at the particle surface (i.e., lipid fluidity and apoA-I conformation) (9). This suggests that changing the phospholipid content of HDL can influence not only the size of the particles but also the functional properties of apoA-I. However, these studies were carried out with rHDL that were heterogeneous in size and in many cases, contained phospholipid species that are not likely to exist in nascent or plasma HDL.

Nonhuman primates fed a diet rich in n–6 and n–3 polyunsaturated fatty acids (PUFA) have decreased plasma HDL and apoA-I concentrations compared to animals fed a diet rich in saturated or monounsaturated fatty acids (10–12). There was also a shift toward smaller HDL subfractions in the PUFA-fed animals as determined by nondenaturing gradient gel electrophoresis (10, 13, 14). When plasma phospholipids isolated from nonhuman primates maintained on an n–3 PUFA diet were incorporated into rHDL, there was a decreased reactivity with LCAT compared to phospholipids isolated from animals fed a lard diet (15). Using defined, synthetic PC species with long chain PUFA in the *sn*-2 position, a decrease was observed in the catalytic efficiency of LCAT, the activation energy of the LCAT reaction, and the stability of apoA-I on rHDL particles (16). There was also an apparent strong association between rHDL apoA-I stability and LCAT activation energy, suggesting that the temperature-dependent step of the LCAT reaction may be sensitive to the strength of the interaction of apoA-I with rHDL PC (16). Based on these results, we hypothesize that there is a decreased interaction of apoA-I with PC species containing long chain PUFA in the *sn*-2 position, which results in alterations in the apoA-I and phospholipid environment and a decrease in LCAT reactivity. However, these previous studies on LCAT reactivity were not performed with homogeneous sized rHDL because of the inherent increased size heterogeneity of rHDL made with PUFA PC compared to POPC.

The goal of the present study was to investigate whether the type of fatty acid in the *sn*-2 position of PC influences the apoA-I/PC interaction and LCAT reactivity using homogeneous sized rHDL. Spectroscopic techniques and monoclonal antibody binding were used to monitor the protein and lipid environment of homogeneous sized rHDL containing synthetic phospholipid species of defined fatty acyl content that mimicked the predominant PC species found in the plasma of animals fed diets enriched in monounsaturated, n-6, and n–3 fatty acids. We found that long-chain PUFA in the *sn*-2 position caused changes in rHDL structure that affected apoA-I stability and conformation as well as influencing the fluidity and hydration of the phospholipid environment. These changes led to a weaker interaction between apoA-I and PC and may be responsible, in part, for the decrease in plasma HDL concentration and subfraction size when diets enriched in PUFAs are consumed.

EXPERIMENTAL PROCEDURES

Materials

The following reagents were purchased from Sigma Chemical Co. (St. Louis, MO); *cis*-5,8,11,14,17-eicosapentaenoic acid (EPA), *cis*-4,7,10,13,16,19-docosahexaenoic acid (DHA), 1-palmitoyl-*sn*-glycero-3-phosphocholine (lysoPC), 4-dimethylaminopyridine, *cis*-5,8,11,14-eicosatetraenoic acid, 1-palmitoyl-2-oleoyl-*sn*-glycero-3-phosphocholine (POPC), 1-palmitoyl-2-linoleoyl-*sn*-3-phosphocholine (PLPC), sodium cholate, dimethyl suberimidate (DMS), *p*-terphenyl, Type II oyster glycogen, and ultrapure guanidine-HCl. Butylated hydroxytoluene, BHT (2,6-di-tert-butyl-4-methylphenol) was purchased from Aldrich Fine Chemicals (Milwaukee, WI). Radiolabeled cholesterol ([7-^{3}H]cholesterol; 21.8 Ci/mmol) was obtained from DuPont/New England Nuclear (Boston, MA). Triethanolamine-HCl was purchased from Fluka Chemicals (Ronkonkoma, NY). 1,6-Diphenyl-1,3,5-hexatriene (DPH) was purchased from Molecular Probes, Inc. (Eugene, OR). Cholesterol was obtained from Nu-Chek Prep, Inc. (Elysian, MN). All other reagents, chemicals, and solvents were purchased from Fisher Scientific Co. (Pittsburgh, PA).

Methods

PC synthesis and rHDL formation. PC species were synthesized from 1-palmitoyl lyso PC and the appropriate fatty acid and purified and characterized as previously described (17,18). The PC species contained 16:0 in the *sn*-1 position and either 18:1 (POPC), 18:2 (PLPC), 20:4 (PAPC), 20:5 n–3 (PEPC), or 22:6 n–3 (PDPC) in the *sn*-2 position.

The cholate dialysis procedure was used to generate rHDL as previously described (4, 16). rHDL complexes had a starting 80:5:1 molar ratio of PC:[^{3}H]cholesterol (50,000 dpm/μg):apoA-I. After extensive dialysis to remove the sodium cholate, the rHDL were subjected to a two-step purification procedure developed to isolate homogeneous size rHDL. The rHDL were adjusted to d 1.221 g/ml with solid KBr and overlayered with d 1.070 g/ml potassium bromide solution. The tubes were then centrifuged in a Beckman SW40 rotor at 40,000 rpm for at least 48 h at 15°C. Samples were removed from the top of the tube by pumping Fluorinert (0.5 ml/min) into the bottom of the tube and fractions were collected (0.5 ml). Fractions were pooled based on absorbance at 280 nm (see Fig. 1). The rHDL were further purified by passing the complexes over two Superdex 200HR HPLC columns (Pharmacia Biotech) connected in series. The particles were eluted at a flow rate of 0.5 ml/min with buffer (10 mm Tris, 140 mm NaCl, 0.01% NaN_3, 0.01% EDTA, pH 7.4). After pooling peak fractions, particle size distribution was determined using 4–30% polyacrylamide gradient gels after electrophoresis for 1400 v·h (19). rHDL were assayed for phospholipid (20), protein (21), and cholesterol (22). rHDL were stored at 4°C under an argon atmosphere.

Crosslinking studies. The number of apoA-I molecules per rHDL particle was determined using the bifunctional crosslinking reagent dimethyl suberimidate (DMS) by a modified version of the Swaney method (23). rHDL (two parts) were incubated with one part freshly prepared DMS solution (20 mg DMS dissolved in 1 ml 1 M triethanolamine HCl, pH 9.7). The mixture was vortexed and incubated at room temperature for 2 h. The re-

action was terminated by the addition of one part 20% SDS solution. After the samples were dried down using a Speed-vac, the pellets were resuspended in running buffer (0.04 M Tris, 0.02 M sodium acetate, 2 mM EDTA, 0.2% SDS, pH 7.4) and subjected to SDS-PAGE electrophoresis using a 4–30% gradient gel (24).

Circular dichroism studies. The stability of rHDL apoA-I was determined by measuring the ellipticity at 222 nm of rHDL in the presence of increasing concentrations of GndHCl as previously described (16). Briefly, 10 μg of rHDL apoA-I was incubated with 0–5 M GndHCl (200 μl final volume) for 72 h at room temperature under an argon atmosphere. The samples and appropriate blanks were scanned from 223 to 221 nm using a 1 mm quartz cell in a Jasco 720 spectropolarimeter (Jasco, Inc., Easton, MD). Five scans of each sample were averaged and the average ellipticity at 222 nm was determined. The ellipticity values (mdeg) were converted to mean residue ellipticity after blank subtraction as previously described (16). The percentage of α-helical content of rHDL apoA-I was calculated by the equation of Chen, Yang, and Martinez (25). The concentration of GndHCl at which denaturation of apoA-I was 50% completed ($D_{1/2}$) and the standard free energy of denaturation (ΔG^o_d) were calculated as previously described (16).

Fluorescence studies. Intrinsic tryptophan fluorescence studies were carried out at an apoA-I concentration of 50 μg/ml. Steady-state emission spectra were obtained using 295 nm exciting light with 2 mm excitation and emission slit widths. Emission was monitored from 310–450 nm at 25°C using an ISS K2 multifrequency phase fluorometer (ISS, Inc.).

Frequency domain fluorometry was used to measure the intrinsic fluorescence lifetimes of the rHDL samples (26). The excitation wavelength was set at 295 nm and emission was observed through a WG320 filter (Schott). The phase and modulation data were obtained over the frequency range of 5–300 MHz. Data analysis was performed by minimizing the reduced chi-square with the ISSL Decay Acquisition Software provided by ISS. The data were fit to a three lifetime component with an error of 0.004 and 0.2 for the modulation and phase data, respectively. A solution of *p*-terphenyl in absolute ethanol was used as a lifetime reference (1.05 ns).

To assess lipid fluidity and degree of hydration of the rHDL samples, fluorescence polarization and lifetime measurements using the probe DPH were used. The DPH probe was dissolved in tetrahydrofuran at 10^{-4} M concentration and added to rHDL solutions containing 25 μg/ml rHDL phospholipid. The molar ratio of PC:probe was 400:1. Lifetime measurements were performed as described above except that the data were fit to a two lifetime component and that a scattering solution of glycogen was used as a lifetime reference. The probe was allowed to equilibrate for at least 15 min at the appropriate temperature before measurements were taken. Polarization measurements were taken at 15°, 25°, 35°C in the L-format (26) with blank subtraction using the following conditions: excitation wavelength = 366 nm, 2 mm slit widths, and KV418 emission filters. The temperature was regulated to ±0.1°C with a circulating water bath.

Monoclonal antibody studies. Competitive solid phase immunoassays were used to assess the binding of monoclonal antibodies to the rHDL. Each antibody used in this study has been described and the epitope on apoA-I was documented (27) with the exception of antibody AI-141.7. The epitope of antibody AI-141.7 was localized to residues 220–242 (L. Curtiss, unpublished observations). The immunoassays were performed as described previously (28). Briefly, human plasma HDL was immoblized onto 96-well Falcon 3911 Microtest III flexible assay plates. rHDL (0.025 ml) were diluted in phosphate-buffered saline containing 3% normal goat serum and added to the wells with a fixed and limiting amount of monoclonal antibody. The plates were incubated overnight at 4°C. After washing the wells, mouse antibody binding to the immobilized antigen was detected by a second 1-h incubation at 37°C with ^{125}I-labeled goat anti-mouse IgG. Data were expressed as B/B_o where B is the cpm bound in the presence of competitor, and B_o is the cpm bound in the absence of competitor. To compare the affinity of the antibodies for the different rHDL, the slopes of log logit-transformed B/B_o ratios were obtained by linear regression analysis.

LCAT incubations. LCAT was purified from fresh recovered human plasma obtained from the Red Cross as described previously (29). SDS-PAGE was used to determine that this procedure resulted in pure LCAT (50 μg/ml). LCAT reactivity was determined as described previously (16). Briefly, LCAT incubations were performed in triplicate in 0.5 ml buffer (10 mM Tris, 140 mM NaCl, 0.01% NaN_3, 0.01% EDTA, pH 7.4) containing: rHDL (0.2 μg cholesterol), 0.6% bovine serum albumin (fatty-acid free), 2 mM β-mercaptoethanol, and 25 ng pure LCAT. Control incubations contained all constituents except LCAT. Tubes were gassed with argon and incubated at 37°C for various times between 10 min and 2 h. Samples were then subjected to lipid extraction and free and esterified cholesterol were separated by thin-layer chromatography and quantified as described previously (29).

RESULTS

Previous studies using rHDL have consistently shown increased size heterogeneity for the rHDL containing PC with long chain PUFA compared with those containing POPC (16, 17). The reason for the increased heterogeneity is unknown but is likely due to differences in apoA-I/PC interaction. As rHDL heterogeneity has an influence on LCAT reactivity and also may influence other physical measurements of rHDL, the objective of this study was to use rHDL that had been purified to apparent size homogeneity.

The rHDL particles used throughout this study were purified to homogeneity by a combination of density gradient ultracentrifugation and gel filtration chromatography as described in the Methods section. Elution of the rHDL complexes was monitored as absorbance at 280 nm. **Figure 1** shows the elution profiles of a representative PDPC rHDL preparation subjected to the purification procedures. The apparent heterogeneity present after the density gradient spin (Fig. 1A) was further reduced after passing the rHDL particles over the Superdex 200 columns (Fig. 1B). The inset to Fig. 1B gives the size distribution of the particles, determined by gradient gel electrophoresis. As can be seen in lane 4, the rHDL were essentially made up of homogeneous sized particles. Results for rHDL containing the other PC species were similar (**Fig. 2**). The chemical compositions and size of the rHDL are shown in **Table 1**. On average, the rHDL containing long chain PUFA had lower PC:apoA-I molar ratios compared to POPC and PLPC rHDL and a slightly smaller size. The Stokes' radius for POPC rHDL was 5.0 nm, whereas the long chain PUFA rHDL ranged in size from 4.5 to 4.6 nm. PLPC rHDL had a Stokes' radius of 4.7 nm. Crosslinking with dimethyl suberimidate showed that all rHDL had two apoA-I per rHDL particle.

ApoA-I stability on the surface of the rHDL particles was determined by incubating rHDL with increasing con-

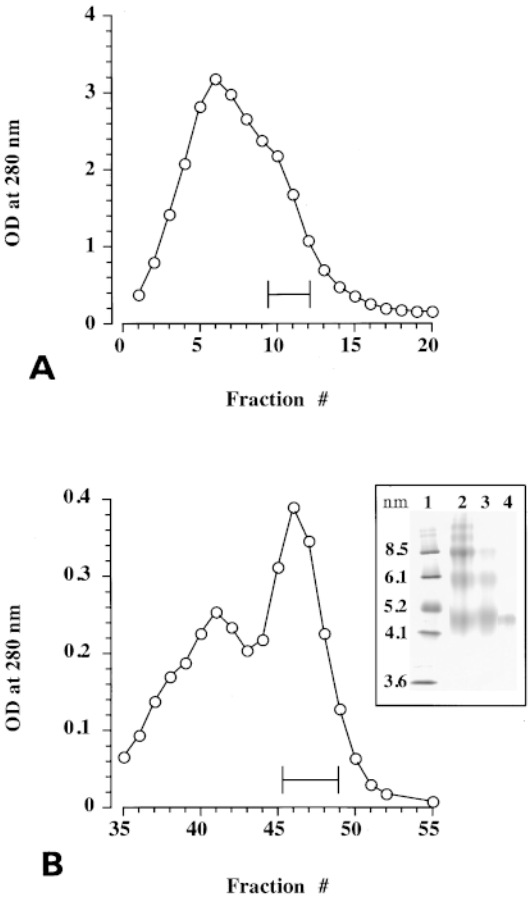

Fig. 1. Elution profile of the rHDL preparation, after density gradient ultracentrifugation (A) and size exclusion chromatography (B). A representative PDPC rHDL preparation is shown. Fractions #9–12 were pooled after density gradient ultracentrifugation spin and applied onto two Superdex 200 HR HPLC columns in series. Fractions #45–49 were pooled after the Superdex run and used for structural studies. The inset shows the 4–30% nondenaturing gradient gel of PDPC rHDL before (lane 2) and after (lane 3) the density gradient spin. Lane 4 shows the final rHDL preparation after chromatography on Superdex 200 HR. Lane 1 contains the following high molecular weight standard proteins along with their hydrated Stokes' radii : thyroglobulin (8.5 nm), ferritin (6.1 nm), catalase (5.2 nm), lactate dehydrogenase (4.1 nm), albumin (3.6 nm).

centrations of GndHCl and monitoring the decrease in ellipticity at 222 nm. The results of a typical experiment are shown in **Fig. 3**. The denaturation curves for the PUFA-containing rHDL were shifted to the left compared to POPC rHDL, indicating that less GndHCl was needed to denature apoA-I on these particles. **Table 2** lists the midpoint of the denaturation curves ($D_{1/2}$), the free energy of denaturation at zero GndHCl concentration (ΔG^0_d), and the α-helical content of apoA-I on rHDL containing the various PC species. POPC rHDL had a greater average $D_{1/2}$ value (2.83 m) compared to the long chain PUFA rHDL (1.57–1.70 m). PLPC rHDL had a $D_{1/2}$ value of 1.95 m. ApoA-I on rHDL containing POPC was thermodynamically more stable (ΔG^0_d = 3.23 kcal/mol) compared to rHDL containing PAPC, PEPC, and PDPC (ΔG^0_d 1.80–2.07 kcal/mol). The ΔG^0_d for PLPC rHDL was intermediate in value (2.90 kcal/mol). There appeared to be a general trend towards decreased apoA-I stability as the number of double bonds in the rHDL PC increased. The percentage of α-helical content of apoA-I was higher for the POPC rHDL (77%) compared to the other rHDL (61–65%). These results, taken together, indicate that apoA-I is more stable on rHDL containing POPC compared to rHDL containing PUFA.

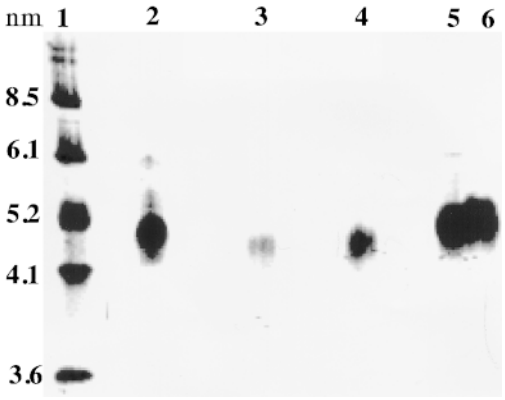

Fig. 2. A 4–30% nondenaturing gradient gel of a representative set of rHDL purified by density gradient ultracentrifugation and Superdex 200 HR column chromatography. Gels were run as described in the Methods section and stained with Coomassie blue followed by destaining. Lane 1 contains high molecular weight standards (see legend to Fig. 1); lane 2, PAPC rHDL; lane 3, PDPC rHDL; lane 4, PEPC rHDL; lane 5, PLPC rHDL; lane 6, POPC rHDL.

The apoA-I tryptophan fluorescence emission spectra for the various rHDL are shown in **Fig. 4**. The emission intensities for the rHDL containing PAPC, PEPC, and PDPC were lower compared to POPC and PLPC rHDL. The wavelength of maximum fluorescence for the rHDL was very similar (328–329 nm). When the rHDL were denatured with 6 m GndHCl, the emission intensities decreased and were indistinguishable (data not shown); the wavelength of maximum fluorescence also increased to 352 nm for all rHDL apoA-I. As it is well recognized that, at equal protein concentrations, higher fluorescence emission intensity indicates a more hydrophobic tryptophan environment, the data suggest that

TABLE 1. Chemical composition of rHDL

rHDL PC	PC : Chol. : Apo A-I	Stokes' Radius
	molar ratio	*nm*
POPC	60 ± 5 : 3.7 ± 0.7 : 1	5.0
PLPC	53 ± 8 : 3.3 ± 0.5 : 1	4.7
PAPC	45 ± 5 : 2.6 ± 0.2 : 1	4.6
PEPC	43 ± 1 : 2.1 ± 0.4 : 1	4.5
PDPC	42 ± 7 : 2.2 ± 0.3 : 1	4.5

Data are the mean ± SEM of three separate preparations of rDHL purified by ultracentrifugation and size-exclusion chromatography. Chemical compositions were determined as outlined in the Methods section. Stokes' radius was determined by electrophoresis using 4–30% polyacrylamide gradient gels. The SEM for all Stokes' radius values was ±0.1. All purified rHDL contained two apoA-I molecules per particle as determined by chemical crosslinking.

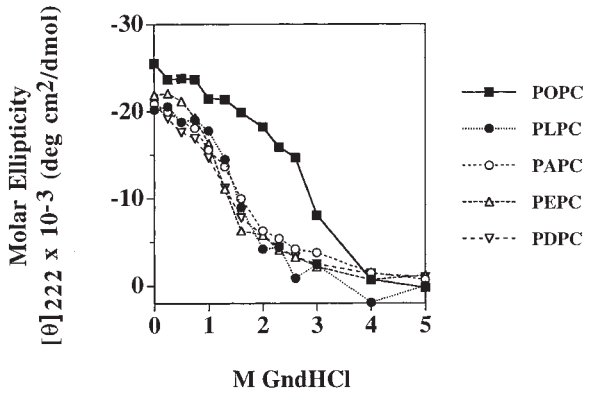

Fig. 3. Guanidine HCl denaturation curves of rHDL monitored by circular dichroism spectroscopy. rHDL (10 μg protein) were adjusted to various final concentrations of guanidine HCl and incubated for 72 h at room temperature under an argon atmosphere before determining ellipticity at 222 nm. Details of the procedure are given in the Methods section.

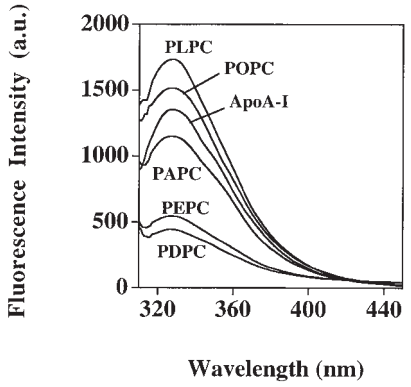

Fig. 4. Tryptophan fluorescence emission spectra of rHDL and lipid-free apoA-I**.** The intrinsic fluorescence emission spectra were recorded from 310–450 nm at 25°C using an excitation wavelength of 295 nm. All samples contained equal amounts of apoA-I (50 μg/ml) in buffer.

the apoA-I tryptophan residues on rHDL containing long-chain PUFA are in a more hydrophilic environment.

Tryptophan fluorescence lifetime measurements were used as another method for detecting differences in the protein environment of the various rHDL. **Figure 5** shows that rHDL containing long chain PUFA PC had shorter average lifetimes compared to rHDL containing POPC and PLPC. As shorter tryptophan lifetime values suggest a more polar environment (26), the data provide further evidence that the apoA-I tryptophan residues on long chain PUFA rHDL existed in a more aqueous environment.

To determine whether there were differences in apoA-I conformation among the rHDL, competitive solid phase immunoassays were used to assess the binding of anti-apoA-I monoclonal antibodies to rHDL. Results from the study of monoclonal antibodies spanning the entire length of apoA-I (**Fig. 6A**) are shown in Fig. 6B as the slopes of the log-logit versus concentration of competitor plots. At the N-terminus there were no apparent differences in the slope values, indicating no differences in conformation in this region of rHDL apoA-I. However, the antibodies to the central region (115.1, 119.1, and 137.1) showed decreased reactivity to PEPC and PDPC rHDL (less negative slope values) compared to PLPC and POPC rHDL. This indicated that these epitope regions were in a different conformation that resulted in decreased affinities of these antibodies for apoA-I on PEPC and PDPC rHDL. PAPC rHDL was intermediate in response to that of PDPC and POPC rHDL. Differences in epitope expression also were observed with antibodies binding at the C-terminus, but the results did not follow a trend that appeared related to the type of fatty acid in the *sn*-2 position of the PC species. These data suggested that the extent of polyunsaturation of the fatty acyl group in the *sn*-2 position of PC consistently altered the conformation of the middle region (amino acids 115–147) of apoA-I on rHDL.

The physical environment of the rHDL phospholipid region was investigated using the fluorescence probe DPH

TABLE 2. Effect of *sn*-2 fatty acyl group of PC on rHDL apoA-I stability

rHDL PC	$D_{1/2}$[a]	$\Delta G°d$[b]	% α-Helix[c]
	(m)	*kcal/mol*	
POPC	2.83 ± 0.07	3.23 ± 0.20	77
PLPC	1.95 ± 0.05	2.90 ± 0.10	63
PAPC	1.70 ± 0.06	2.07 ± 0.29	61
PEPC	1.57 ± 0.03	1.80 ± 0.21	65
PDPC	1.83 ± 0.09	2.03 ± 0.38	62
ApoA-I	1.05 ± 0.05	2.40 ± 0.10	37

[a] Concentration of GndHCl needed to denature 50% of rHDL apoA-I (mean ± SEM, n = 3).

[b] Standard change in free energy of denaturation at zero GndHCl (mean ± SEM, n = 3).

[c] Percentge of α-helical content calculated from the mean residue ellipticity at 222 nm using the formula of Chen et al. (25). Data are from a representative set of rHDL.

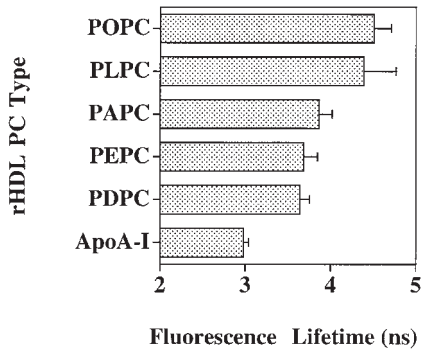

Fig. 5. Average tryptophan fluorescence lifetime of rHDL and lipid-free apoA-I. Frequency domain fluorometry was used to measure the intrinsic fluorescence lifetimes. Samples contained 50 μg/ml apoA-I in buffer. Phase and modulation data were obtained over the frequency range 5–300 MHz at 25°C. The average lifetime was calculated by the following equation: $\tau = \Sigma_i f_i \tau_i$, where f_i and τ_i represent the fractional contribution and resolved lifetime, respectively. Data were subjected to a three-exponential analysis and represent the mean ± SEM of three separate preparations of rHDL.

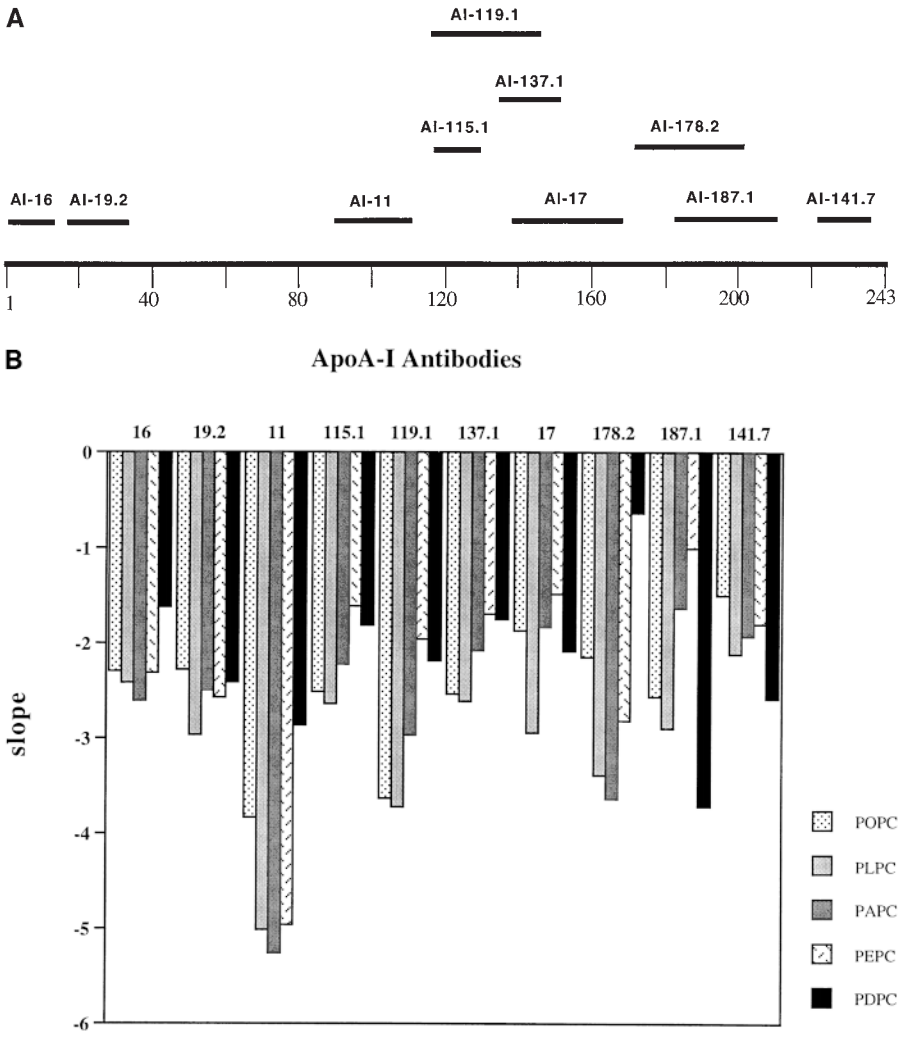

Fig. 6. Linear model of apoA-I primary structure (A) with the monoclonal antibody epitope assignments indicated by the apoA-I amino acid residues in parentheses: AI-16 (1–15), AI-19.2 (19–31), AI-11 (96–111), AI-115.1 (115–126), AI-119.1 (119–144), AI-137.1 (137–147), AI-17 (143–165), AI-178.2 (178–200), AI-187.1 (187–210), AI-141.7 (220–242). Competitive solid-phase binding assay for rHDL (B). Slopes were determined by linear regression analysis of log-logit plots (see Methods section). Data shown are representative of assays performed with the antibodies on three different preparations of rHDL.

to measure PC fluidity and to assess the relative hydration of the bilayer environment. Steady-state DPH fluorescence polarization was used to measure the fluidity of the rHDL bilayer. Lower polarization values indicate a more fluid environment resulting from increased motions of the phospholipid fatty acyl chains. Over the temperature range studied, the polarization curves for all PUFA containing rHDL species were lower compared to POPC rHDL (**Fig. 7**), indicating a more fluid environment in the PC of those rHDL.

It has been reported that the fluorescence lifetime of DPH can be used as an indicator for the degree of hydration of lipid bilayers (30). **Figure 8** shows that there was an apparent linear decrease in DPH fluorescence lifetime with increasing unsaturation at the *sn*-2 position of PC ($r^2 = 0.89$). These findings are consistent with previous studies using large unilamellar vesicles which contain no cholesterol or protein (30). These studies suggest that the decrease in DPH lifetime in rHDL containing PC with long chain PUFA was due to an increased hydration of the phospholipid environment.

Figure 9 shows the LCAT reactivity of the various rHDL species. The rHDL containing PAPC, PEPC, and PDPC resulted in less cholesteryl ester formation compared to POPC and PLPC rHDL, demonstrating that rHDL of homogeneous size containing long chain PUFA were less reactive with LCAT.

DISCUSSION

The purpose of this study was to investigate whether the type of fatty acid in the *sn*-2 position of PC influences rHDL apoA-I/PC interactions. We have previously found that there is a strong association between rHDL apoA-I stability and LCAT activation energy, suggesting that the

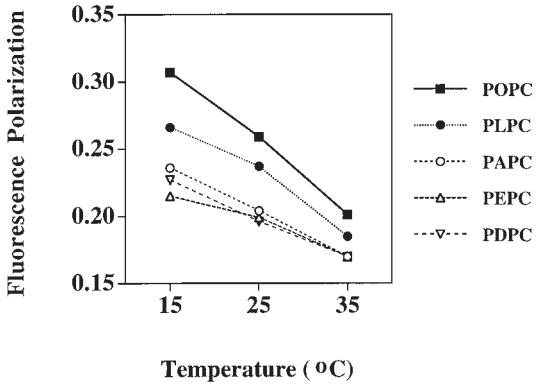

Fig. 7. DPH fluorescence polarization as a function of temperature. DPH was incorporated into the lipid bilayer of rHDL at a molar ratio of PC:probe = 400:1.

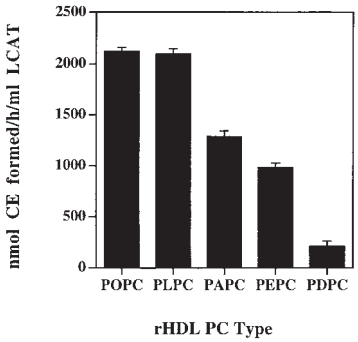

Fig. 9. LCAT reactivity of rHDL. Details of the LCAT assays are provided in the Methods section. CE formation was kept in the linear range (<25% CE formation) by adjusting the incubation times for each rHDL sample. Data represents the mean ± SEM for a set of rHDL assayed in triplicate.

temperature-dependent step of the LCAT reaction may be sensitive to the strength of the interaction of apoA-I with rHDL PC (16). Using homogeneous populations of rHDL containing defined PC species, we analyzed the protein and lipid environments to determine how different PC species influence rHDL structure. We found that long chain PUFA in the *sn*-2 position of PC causes changes in rHDL structure affecting apoA-I stability and conformation as well as influencing the fluidity and hydration of the phospholipid environment. We conclude that the structural changes observed with the long chain PUFA species result in a weaker interaction between rHDL apoA-I and PC.

One of the objectives of this study was to use rHDL that had been purified to apparent size homogeneity. It is well established that rHDL heterogeneity can have an influence on LCAT reactivity and other physical measurements of rHDL (7). We have consistently observed more size heterogeneity and larger subpopulations for rHDL with PC species containing long chain PUFA compared to POPC and PLPC, even though the starting ratio of PC:cholesterol:apoA-I is the same for each rHDL. The difference in intrinsic properties of PC with long chain PUFA may lead to more stable interactions between PC and apoA-I on larger rHDL containing three or four molecules of apoA-I compared to those on smaller rHDL containing two apoA-I molecules per particle. Our purification of rHDL to a single homogeneous size was achieved through a combination of density gradient ultracentrifugation and size exclusion chromatography. On average, homogeneous sized rHDL particles containing two apoA-I molecules and long chain PUFA (PAPC, PEPC, PDPC) had lower PC:apoA-I molar ratio compared to POPC (Table 1), resulting in a slightly reduced Stokes' radii for these particles. The most likely explanation for these findings is that PC containing long chain PUFA have an increased molecular surface area compared to POPC. Increasing the chain length and the number of double bonds results in larger molecular surface areas as determined by monolayer force–area isotherms of purified PC species (18, 31). Thus, apoA-I in any given conformation would be able to bind fewer PC molecules when long chain PUFA are present in the *sn*-2 position of PC compared to POPC.

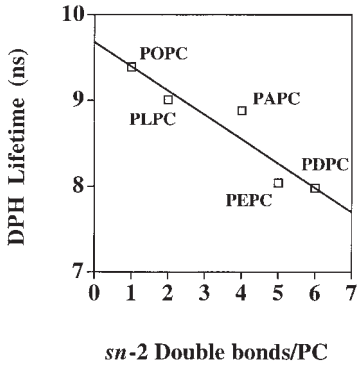

Fig. 8. Plot of DPH fluorescence lifetime (major component) versus the number of *sn*-2 double bonds in rHDL PC. Each point represents the mean of the major lifetime component of DPH from two sets of rHDL. Lifetimes were calculated from a two-exponential analysis of the phase and modulation data over the frequency range 2–150 MHz at 25°C. The line of best fit ($r^2 = 0.89$), determined by linear regression analysis, is shown.

The structural stability of rHDL apoA-I was assessed by denaturation with GndHCl. We found that PC containing PUFA decreased the stability of rHDL apoA-I compared to POPC (Table 2). There was also a slight reduction in α-helical content with the incorporation of PUFA into PC. However, the differences in α-helical content most likely do not contribute to the decreased stability, as it has been found that there is no relationship between rHDL apoA-I α-helical content and stability (32, 33). The decrease in apoA-I stability on rHDL PC containing PUFA likely results from the increased surface area of the PC (as discussed above) and the increased polarity of the *sn*-2 fatty acyl chain. We observed a trend towards decreased rHDL apoA-I stability as the number of *sn*-2 double bonds increased in PC (Table 2). It is well documented that the interaction of apoA-I with PC stabilizes its structure resulting in a higher α-helical content and increased resistance to denaturation by guanidine HCl or heat treatment (34). Both increased PC surface area and *sn*-2 fatty acyl chain

polarity may lead to a less stable interaction of the hydrophobic face of apoA-I amphipathic helices with the more polar and extended PUFA chains.

Investigation into apoA-I structure on the rHDL made with the various PC species was studied using fluorescence spectroscopy and monoclonal antibodies. We found that the intrinsic tryptophan fluorescence emission intensity and lifetimes were decreased for the rHDL containing PAPC, PEPC, and PDPC compared to POPC and PLPC (Figs. 4 and 5). These results suggest that the tryptophan residues in apoA-I complexed with PC species containing long chain PUFA were exposed to a more aqueous environment. The apoA-I tryptophan residues are located mainly at the N-terminus (amino acids 8, 50, 72, 108). However, monoclonal antibody competition studies showed no differences in epitope expression at the N-terminus for the rHDL studied (Fig. 6). Thus, it appears that the differences in the fluorescence measurements are not due to major conformational changes in apoA-I at the N-terminal region, but possibly result from changes in the PC fatty acyl environment. The most likely explanation that would cause a decreased fluoresence intensity without a shift in emission wavelength would be due to an increased presence of water in the lipid bilayer. Slater et al. (35) have shown that a decreased fluorescence intensity of a membrane fluorescent probe in the presence of increased numbers of double bonds was due to an increased amount of water in the fluorophore excited state solvent cage.

We found that rHDL containing long chain PUFA had decreased fluorescence polarization values compared to POPC rHDL (Fig. 7). Because lower polarization values indicate a more fluid environment, due to increased motions of the PC fatty acyl chains, we conclude that the phospholipid environment of the rHDL containing long chain PUFA is more fluid than that of POPC rHDL. We also found, using the fluorescence probe DPH, that there is an apparent linear decrease in DPH lifetime as the number of *sn*-2 double bonds increases (Fig. 8). These results are consistent with previous studies using large unilamellar vesicles (30) and demonstrate that the decrease in fluorescence lifetime with increasing number of double bonds reflects an intrinsic property of PC, which is not affected when protein and cholesterol are present in the rHDL particle. It is widely accepted that a decrease in the fluorescence lifetime of DPH occurs due to an increased hydration of the lipid bilayer (30), presumably because of fluorophore excited state–water interactions (36). In addition, PUFA can generate packing "defects" in membrane systems, due to *trans*-gauche isomerization of the fatty acyl chains (37), leading to increased water in membrane systems. The data taken together, are consistent with the hypothesis that an increased presence of water in the bilayer of PUFA-containing rHDL apoA-I may alter the conformation of apoA-I by affecting its ability to associate with PC, thus resulting in a weaker apoA-I/PC interaction.

While there were no apparent conformational changes at the N-terminus of apoA-I on PUFA-containing rHDL compared to POPC rHDL, we did detect changes over the central region of apoA-I (Fig. 6). The monoclonal antibodies used over this region corresponded to amino acids 115–147. This region has been implicated in LCAT activation (28). One could speculate that a conformational change in apoA-I over this region could result in changes in LCAT reactivity and activation energy observed for PUFA containing rHDL (16) by altering LCAT binding to the particle surface and/or influencing access of the fatty acid chain to the active site.

We propose the following model of rHDL particle structure to account for our experimental observations. The fatty acyl region of rHDL containing long chain PUFA is more fluid, more hydrophilic, and occupies a greater surface area per molecule than the fatty acyl region of rHDL containing POPC. This leads to a weakened interaction between apoA-I α-helices and the fatty acyl region of the polyunsaturated PC, resulting in decreased stability of apoA-I on these rHDL. The decreased interaction between apoA-I and PC may also result in greater intra-helical interaction between adjacent α-helical regions of apoA-I to help stabilize the regions of apoA-I that are not tightly associated with the fatty acyl region of PC. The increased surface area and fluidity of the polyunsaturated PC species results in fewer PC molecules per rHDL particle.

The physiological consequences of this mechanism may be the reduced conversion of nascent, discoidal HDL to mature spherical HDL by LCAT and a greater fraction of the destabilized apoA-I that leaves nascent particles and becomes hypercatabolized. Lipid-free apoA-I has been shown to be hypercatabolized once it leaves an HDL particle (38, 39). This would lead to a faster catabolic rate (FCR) for animals fed a PUFA diet. Several studies have shown a higher FCR for animals fed PUFA (40–43). This may lead to the observed lower HDL and apoA-I concentrations and smaller HDL subfractions in plasma of animals fed a diet rich in PUFA (10–13).

These studies were supported by an Institutional NRSA Training grant HL-07115 (KWH) and Public Health Service grants HL-49373 (JSP) and HL-43815 (LKC) from the National Institutes of Health. The circular dichroism and fluorescence spectroscopy instruments were supported by the North Carolina Biotechnology Center. The authors gratefully acknowledge the excellent technical assistance of Kathi Richards, and the helpful discussions of Drs. Dong Lyles (Wake Forest University) and Fred Schroeder (Texas A&M) regarding fluorescence spectroscopy.

Manuscript received 14 May 1998 and in revised form 4 August 1998.

REFERENCES

1. Segrest, J. P., M. K. Jones, H. De Loof, C. G. Brouillette, and Y. V. Venkatachalapathi. 1992. The amphipathic helix in the exchangeable apolipoproteins: a review of secondary structure and function [Review]. *J. Lipid Res.* **33:** 141–166.
2. Segrest, J. P., R. L. Jackson, J. D. Morrisett, and A. M. Gotto, Jr. 1974. A molecular theory of lipid–protein interactions in the plasma lipoproteins. *FEBS Lett.* **38:** 247–258.
3. Tall, A. R., and D. M. Small. 1980. Body cholesterol removal: role of plasma high-density lipoproteins. *Adv. Lipid Res.* **17:** 1–51.
4. Matz, C. E., and A. Jonas. 1982. Micellar complexes of human apolipoprotein A-I with phosphatidylcholines and cholesterol prepared from cholate–lipid dispersions. *J. Biol. Chem.* **257:** 4535–4540.

5. Johnson, F. L., J. Babiak, and L. L. Rudel. 1986. High density lipoprotein accumulation in perfusates of isolated livers of African green monkeys. Effects of saturated versus polyunsaturated dietary fat. *J. Lipid Res.* **27:** 537–548.
6. Wald, J. H., E. Coormaghtigh, J. De Meutter, J. M. Ruysschaert, and A. Jonas. 1990. Investigation of the lipid domains and apolipoprotein orientation in reconstituted high density lipoproteins by fluorescence and IR methods. *J. Biol. Chem.* **265:** 20044–20050.
7. Jonas, A., K. E. Kezdy, and J. H. Wald. 1989. Defined apolipoprotein A-I conformations in reconstituted high density lipoprotein discs. *J. Biol. Chem.* **264:** 4818–4824.
8. Zorich, N. L., K. E. Kezdy, and A. Jonas. 1987. Properties of discoidal complexes of human apolipoprotein A-I with phosphatidylcholines containing various fatty acid chains. *Biochim. Biophys. Acta.* **919:** 181–189.
9. Jonas, A., N. L. Zorich, K. E. Kezdy, and W. E. Trick. 1987. Reaction of discoidal complexes of apolipoprotein A-I and various phosphatidylcholines with lecithin:cholesterol acyltransferase. Interfacial effects. *J. Biol. Chem.* **262:** 3969–3974.
10. Parks, J. S., J. A. Martin, B. L. Sonbert, and B. C. Bullock. 1987. Alteration of high density lipoprotein subfractions of nonhuman primates fed fish-oil diets. Selective lowering of HDL subfractions of intermediate size and density. *Arteriosclerosis.* **7:** 71–79.
11. Wolfe, M. S., J. S. Parks, T. M. Morgan, and L. L. Rudel. 1993. Childhood consumption of dietary polyunsaturated fat lowers risk for coronary artery atherosclerosis in African green monkeys. *Arterioscler. Thromb.* **13:** 863–875.
12. Thornburg, J. T., J. S. Parks, and L. L. Rudel. 1995. Dietary fatty acid modification of HDL phospholipid molecular species alters lecithin:cholesterol acyltransferase reactivity in cynomolgus monkeys. *J. Lipid Res.* **36:** 277–289.
13. Babiak, J., F. T. Lindgren, and L. L. Rudel. 1988. Effects of saturated and polyunsaturated dietary fat on the concentrations of HDL subpopulations in African green monkeys. *Arteriosclerosis.* **8:** 22–32.
14. Schonfeld, G., W. Patsch, L. L. Rudel, C. Nelson, M. Epstein, and R. E. Olson. 1982. Effects of dietary cholesterol and fatty acids on plasma lipoproteins. *J. Clin. Invest.* **69:** 1072–1080.
15. Parks, J. S., B. C. Bullock, and L. L. Rudel. 1989. The reactivity of plasma phospholipids with lecithin:cholesterol acyltransferase is decreased in fish oil-fed monkeys. *J. Biol. Chem.* **264:** 2545–2551.
16. Parks, J. S., and A. K. Gebre. 1997. Long chain polyunsaturated fatty acids decrease the stability of recombinant high density lipoprotein apoA-I and the activation energy of lecithin:cholesterol acyltransferase reaction. *J. Lipid Res.* **38:** 266–275.
17. Parks, J. S., T. Y. Thuren, and J. D. Schmitt. 1992. Inhibition of lecithin:cholesterol acyltransferase activity by synthetic phosphatidylcholine species containing eicosapentaenoic acid or docosahexaenoic acid in the *sn*-2 position. *J. Lipid Res.* **33:** 879–887.
18. Parks, J. S., and T. Y. Thuren. 1993. Decreased binding of apoA-I to phosphatidylcholine (PC) monolayers containing 22:6 n–3 in the *sn*-2 position. *J. Lipid Res.* **34:** 779–788.
19. Rainwater, D. L., D. W. Andres, A. L. Ford, W. F. Lowe, P. J. Blanche, and R. M. Krauss. 1992. Production of polyacrylamide gradient gels for the electrophoretic resolution of lipoproteins. *J. Lipid Res.* **33:** 1876–1881.
20. Fiske, C. H., and Y. SubbaRow. 1925. Colorimetric determination of phosphorus. *J. Biol. Chem.* **66:** 357–400.
21. Lowry, O. H., N. J. Rosebrough, A. L. Farr, and R. J. Randall. 1951. Protein measurement with the Folin phenol reagent. *J. Biol. Chem.* **193:** 265–275.
22. Auerbach, B. J., J. S. Parks, and D. Applebaum-Bowden. 1990. A rapid and sensitive micro-assay for the enzymatic determination of plasma and lipoprotein cholesterol. *J. Lipid Res.* **31:** 738–742.
23. Swaney, J. B. 1986. Use of cross-linking reagents to study lipoprotein structure. *Methods Enzymol.* **128:** 613–626.
24. Auerbach, B. J., and J. S. Parks. 1989. Lipoprotein abnormalities associated with lipopolysaccharide-induced lecithin: cholesterol acyltransferase and lipase deficiency. *J. Biol. Chem.* **264:** 10264–10270.
25. Chen, Y., J. T. Yang, and H. M. Martinez. 1972. Determination of the secondary structures of proteins by circular dichroism and optical rotatory dispersion. *Biochemistry.* **11:** 4120–4131.
26. Lackowicz, J. R. Principles of Fluorescence Spectroscopy, Plenum Press, New York, NY.
27. Curtiss, L. K., and C. L. Banka. 1996. Selection of monoclonal antibodies for linear epitopes of an apolipoprotein yields antibodies with comparable affinity for lipid-free and lipid-associated apolipoprotein. *J. Lipid Res.* **37:** 884–892.
28. Sorci-Thomas, M. G., L. Curtiss, J. S. Parks, M. J. Thomas, and M. W. Kearns. 1997. Alteration in apolipoprotein A-I 22-mer repeat order results in a decrease in lecithin:cholesterol acyltransferase reactivity. *J. Biol. Chem.* **272:** 7278–7284.
29. Miller, K. R., J. Wang, M. Sorci-Thomas, R. A. Anderson, and J. S. Parks. 1996. Glycosylation structure and enzyme activity of lecithin:cholesterol acyltransferase from human plasma, HepG2 cells, and baculoviral and Chinese hamster ovary cell expression systems. *J. Lipid Res.* **37:** 551–561.
30. Ho, C., S. J. Slater, and C. D. Stubbs. 1995. Hydration and order in lipid bilayers. *Biochemistry.* **34:** 6188–6195.
31. Evans, R. W., M. A. Williams, and J. Tinoco. 1987. Surface areas of 1-palmitoyl phosphatidylcholines and their interactions with cholesterol. *Biochem. J.* **245:** 455–462.
32. Sparks, D. L., W. S. Davidson, S. Lund-Katz, and M. C. Phillips. 1993. Effect of cholesterol on the charge and structure of apolipoprotein A-I in recombinant high density lipoprotein particles. *J. Biol. Chem.* **268:** 23250–23257.
33. Sparks, D. L., W. S. Davidson, S. Lund-Katz, and M. C. Phillips. 1995. Effects of the neutral lipid content of high density lipoprotein on apolipoprotein A-I structure and particle stability. *J. Biol. Chem.* **270:** 26910–26917.
34. Sparks, D. L., S. Lund-Katz, and M. C. Phillips. 1992. The charge and structural stability of apolipoprotein A-I in discoidal and spherical recombinant high density lipoprotein particles. *J. Biol. Chem.* **267:** 25839–25847.
35. Slater, S. J., M. B. Kelly, F. J. Taddeo, C. J. Ho, E. Rubin, and C. D. Stubbs. 1994. The modulation of protein kinase C activity by membrane lipid bilayer structure. *J. Biol. Chem.* **269:** 4866–4871.
36. Mitchell, D. C., and B. J. Litman. 1994. Effect of ethanol on metarhodopsin II formation is potentiated by phospholipid polyunsaturation. *Biochemistry.* **33:** 12752–12756.
37. Trauble, H. 1971. The movement of molecules across lipid membranes: a molecular theory. *J. Membr. Biol.* **4:** 193–208.
38. Horowitz, B. S., I. J. Goldberg, J. Merab, T. M. Vanni, R. Ramakrishnan, and H. N. Ginsberg. 1993. Increased plasma and renal clearance of an exchangeable pool of apolipoprotein A-I in subjects with low levels of high density lipoprotein cholesterol. *J. Clin. Invest.* **91:** 1743–1752.
39. Shepherd, J., A. M. Gotto, Jr., O. D. Taunton, M. J. Caslake, and E. Farish. 1977. The in vitro interaction of human apolipoprotein A-I and high density lipoproteins. *Biochim. Biophys. Acta.* **489:** 486–501.
40. Chong, K. S., R. J. Nicolosi, R. F. Rodger, D. A. Arrigo, R. W. Yuan, J. J. MacKey, and P. N. Herbert. 1987. Effect of dietary fat saturation on plasma lipoproteins and high density lipoprotein metabolism of the rhesus monkey. *J. Clin. Invest.* **79:** 675–683.
41. Parks, J. S., and L. L. Rudel. 1982. Different kinetic fates of apolipoproteins A-I and A-II from lymph chylomicra of nonhuman primates. Effect of saturated versus polyunsaturated dietary fat. *J. Lipid Res.* **23:** 410–421.
42. Brousseau, M. E., E. J. Schaefer, A. F. Stucchi, J. Osada, D. B. Vespa, J. M. Ordovas, and R. J. Nicolosi. 1995. Diets enriched in unsaturated fatty acids enhance apolipoprotein catabolism but do not affect either its production or hepatic mRNA abundance in cynomolgus monkeys. *Atherosclerosis.* **115:** 107–119.
43. Stucchi, A. F., L. K. Hennessy, D. B. Vespa, E. J. Weiner, J. Osada, J. M. Ordovas, and R. J. Nicolosi. 1991. Effect of corn and coconut oil-containing diets with and without cholesterol on high density lipoprotein apoprotein A-I metabolism and hepatic apoprotein A-I mRNA levels in cebus monkeys. *Arterioscler. Thromb.* **11:** 1719–1729.